

Decoupling the effect of membrane thickness and CNC concentration in PVA based nanocomposite membranes for CO₂/CH₄ separation

Zaib Jahan^{a,b}, Muhammad Bilal Khan Niazi^b, May-Britt Hägg^a, Øyvind Weiby Gregersen^{a,*}

^aDepartment of Chemical Engineering, Norwegian University of Science and Technology, Norway

^bDepartment of Chemical Engineering, School of Chemical and Materials Engineering, National University of Sciences and Technology, Islamabad, Pakistan

Abstract

The effect of the viscosity of the casting suspension on membrane morphology and thickness has been investigated for polyvinyl alcohol (PVA)/ crystalline nanocellulose (CNC) nanocomposite membranes used for CO₂/CH₄ separation. Different concentrations of CNC suspended in dissolved PVA affected the viscosities of resulting suspensions. A methodology was developed to make equal viscosity suspensions with variable CNC content. SEM micrographs show that by increasing the concentration of CNC in PVA, the thickness of the selective layer increased. However, equal thickness was achieved by water dilution for viscosity adjustment. The overall objective of this work was to find the real optimum concentration of CNC in PVA for CO₂/CH₄ separation independent of the membrane thickness. Furthermore, the effect of the relative humidity (RH) and feed pressure on the selectivity and permeability of the membranes were also investigated as part of this study. For 1.5 % CNC in PVA with pH 9 in the casting suspension, tested at feed pressure of 5 bar, CO₂/CH₄ selectivity was up to 39 and the achieved permeance was 0.27 m³(STP)/ (m² h bar). Above this concentration of CNC, the CO₂ permeation and selectivity decreased. It was also observed that increasing pressure caused a decrease in the performance of the membranes for CO₂ capture in terms of both permeation and selectivity. Moreover, increasing RH causes increasing in CO₂ permeation and selectivity.

Keywords:

Crystalline nanocellulose (CNC); Polyvinyl alcohol (PVA); Nanocomposite membranes;
Facilitated transport membranes (FTM); Biogas upgrading.

*Corresponding Author: oyvind.w.gregersen@ntnu.no (Øyvind Weiby Gregersen)

Tel.: +47-73594029

Postal address: Department of Chemical Engineering, Norwegian University of Science and
Technology, Norway

Highlights:

- 1) Thickness of the selective layer increased with CNC concentration in membranes.
- 2) Thickness of membranes was optimized by water dilution for viscosity adjustment.
- 3) The swelling of nanocomposite membranes increased by the addition of CNC
- 4) Nanocomposite membranes with 1.5% CNC showed best permeation results
- 5) Higher relative humidity increases the CO₂ permeation and selectivity

1. Introduction

CO₂ is the most dominating anthropogenic greenhouse gas. Release of CO₂ into the atmosphere is responsible for 77% of human contribution towards the greenhouse effect [1]. Combustion of fossil fuels to meet energy demands is one of the major sources of CO₂ emission. Release of CO₂ from burning fossil fuel and certain industries (cement, steel) have increased 61% from year 1990 till 2013 [2]. In order to cope with the environmental consequences of greenhouse gas (GHG) emissions, a transition towards renewable energies is required. The use of renewable energy as a source of alternative electricity generation is predicted to increase at 3.1% per year from 2008 to 2035 [3]. Biogas is a potential renewable energy source. It mainly consists of CH₄ (50-75) % and CO₂ (25-50) %. Furthermore, it can be upgraded by separating CO₂ from CH₄. The upgraded biogas must contain at least 95% CH₄. CH₄ in the form of compressed natural gas can be used as vehicle fuel, for electricity generation, and for domestic ovens and furnaces. CH₄ based fuels are considered more environmental friendly than other fossile fuels [4].

Carbon Capture Use and Storage (CCUS) is indicated as the technology with the highest potential to reduce CO₂ emission into the atmosphere. CCUS is equally applicable for both post-combustion and pre-combustion CO₂ capture. CO₂ separated from flue gases can be used in Enhanced Oil Recovery (EOR) [2, 5].

Among all post combustion CO₂ technologies amine absorption and cryogenic processes are currently commercially available. Recently, it has been investigated that CO₂ – nanofluid absorption systems is a promising technique particularly for pollution control. However, low absorption capabilities and high energy consumption is still a challenge for this technique [6]. Membrane technology is an emerging green technology that offers several advantages over other commercially available technologies. A membrane is a thin barrier usually coated on a support that selectively allows CO₂ to pass from feed side to permeate side. Simplicity,

energy efficiency and environment friendliness, low capital cost, easy to operate, better utilization of space and suitability for remote location applications are a few advantages of membrane technology [7]. However, there are some challenges that limit the applications of membrane systems in CO₂ capture [8]. When determining the performance of membrane systems, permeability and selectivity parameters are of major importance. In order to make membranes commercially viable and compete with conventional amine absorption, a commercial scale membrane module with high CO₂ permeance and high selectivity of CO₂/N₂ for post-combustion and CO₂/CH₄ for pre-combustion applications is required. The scaling up is never a linear process based on lab data, and the engineering of the commercial process will also be of major importance.

During the last decade membrane separation technology has gained much attention as an emerging technology for CO₂ capture. Different types of materials like ceramics, carbon, polymers and ionic liquids have been investigated for their CO₂ separation performance. Zhien et al. has proposed that membrane separation combined with gas absorption is a good potential solution to absorb acidic gases. He has used number of amine based solvents and mixed amine solvents combined with hydrophobic hollow fiber membranes [9].

Polymeric membranes seem suitable to be used at commercial scale due to their easy fabrication, low cost, and reasonably high membrane performance [10, 11]. This article focuses on optimization of the performance of facilitated transport membranes (FTM). Facilitated transport membranes are polymeric membranes in which a moving carrier is embedded into a polymer matrix. CO₂ transport through FTM mainly occurs by the solution diffusion and carrier-mediated mechanism.

CO₂ reversibly reacts with water which acts as a carrier molecule. Bicarbonate (HCO₃⁻) is formed and hence selectively permeate through the membrane. Un-reactive gases such as, N₂ and CH₄ permeates exclusively by the solution diffusion mechanism [12].

Transfer of gas through the membrane may be described by the mass flux 'j' of component A through the membrane. Mass flux is defined by using Fick's law of diffusion [13].

$$J = -D \frac{dc}{dx} \quad (1)$$

Where, J is mass flux, D is diffusion coefficient and dc/dx is the driving force in terms of concentration gradient. Equation (1) can be further modified for mass flux at the liquid gas interface;

$$J_A = \frac{D_A}{L} (C_{A,0} - C_{A,L}) \quad (2)$$

Where L is the membrane thickness and the driving force is the concentration difference at the gas liquid interface. When considering carrier facilitated transport through membranes, equation (2) gets more complex. In carrier facilitated transport, carriers have an additional contribution towards the diffusion of one specific component in the feed gas. Thus, total flux in this case will be sum of Fickian diffusion and carrier-mediated diffusion.

$$J_A = \frac{D_A}{L} (C_{A,0} - C_{A,L}) + \frac{D_{A,C}}{L} (C_{AC,0} - C_{AC,L}) \quad (3)$$

The first term describes Fickian diffusion whereas second term of the equation describes carrier-mediated diffusion. Carrier mediated diffusion is a complicated phenomenon but has been explained in detail in literature [14]. From equation (3), it is clear that facilitated transport can be maximized by reducing the thickness of the membrane and by increasing the selectivity of carrier molecules for one of the components.

In order to enhance membrane performance, considerable research has been focused on innovative membrane materials and optimization of system parameters and structure designs. When it comes to large scale applications membrane thickness is also a critical parameter that affects both membrane performance and cost effectiveness. Mensitieri et al. investigated the

transport of pure oxygen in dry and water saturated Kapton polyimide films of different thickness (13-50 μm). Experiments were conducted by using three different configurations; gas-membrane-gas configuration, liquid-membrane-liquid configuration (electrochemical cell) and high pressure gas sorption technique. In dry tests both solubility and average diffusivity were found to increase with thickness, while for water saturated films an increase in diffusivity caused a decrease in solubility. The behavior of films in dry and saturated conditions has been explained in terms of film morphologies. Crystallinity, porosity and free volume were three major factors affecting the transport through Kapton. However the effect of free volume was found to be much less pronounced of water saturated conditions [15].

Shen et al. fabricated the P84 polyimide membranes with thickness ranging from 6 to 310 μm using spin coating to investigate the effect of membrane thickness on the gas transport properties. SEM was used to measure membrane thickness. The study shows that the permeability of single gases (He , N_2 , O_2 , and CO_2) increases with increasing membrane thickness. Whereas, the selectivity of gas pairs (O_2/N_2 , He/CO_2 , CO_2/N_2 , and He/O_2) is nearly independent of the membrane thickness [16].

Firpo et al. described the technique to prepare PDMS membranes to determine the thickness dependence of the permeability for CO_2 and He . SEM/FIB measurements were used for thickness control. The study showed that permeability became thickness dependent below some tens of micrometers. Flux models based on interface reaction were applied to quantitatively describe the thickness-dependence of the permeability. The model allows determining the rate constants of the surface reactions for CO_2 and He on PDMS. However, by reducing the membrane thickness below 200 nm, both permeability and selectivity change, indicating Knudsen diffusion as the main flux mechanism responsible for permeation. In this range of thickness, SEM images revealed membrane defects [17].

Koops et al. investigated that pervaporation selectivity of polysulfone (PSf), poly(vinyl chloride) (PVC), and polyacrylonitrile (PAN) decreases with increase in

membrane thickness below a value of about 15 μm [18]. Huang and Paul investigated the effect of membrane thickness (0.4 to 60 μm) of the three different glassy polymers polysulfone, poly (2,6-dimethyl-1,4- phenylene oxide and polyimide for oxygen, nitrogen and methane permeabilities for more than one year. They found that the effect of aging became greater for thinner films resulting in a decrease in permeability [19]. Ahmad et al. investigated the effect of thickness on morphology and permeation of CO_2/N_2 gases in asymmetric flat sheet polyetherimide membranes for non-wetted system. SEM was used to investigate membrane morphology. The permeability decreased with increasing membrane thickness above 300 μm [20].

Nanocellulose has been used as filler in the polymeric matrix for different membrane applications [21]. Cellulose is the most abundantly available biodegradable and renewable natural polymer in the ecosystem. Defect free rod like nanocrystals are produced as a result of acid hydrolysis of cellulose [22, 23]. Cellulose nano crystals (CNC) have unique properties such as low density, high aspect ratio, high mechanical strength and high specific surface area [24-26]. CNC from wood is 3-5 nm wide and 100-200 nm long [22]. When nanocomposite films of CNC in PVA are subjected to humid environment they show high degree of swelling. The degree of swelling varies with CNC concentration [27]. This feature makes CNC an interesting material to use as filler in water swollen polymeric membranes to facilitate the transport of CO_2 [21, 28]. However, increase in the concentration of nano fillers in polymeric solutions will result in an increase in the viscosity of the suspensions. The resultant suspensions with high viscosity gives thicker and non-uniform membranes after dip coating and hence results in a drop of membrane performance after addition of a certain amount of nano fillers.

In this work equal viscosity suspensions of CNC ranging from (0.5% - 4%) CNC wt./wt. PVA were made. Membranes cast from these suspensions were examined for their

morphology and thickness of the selective layer. Permeation tests were conducted to optimize the concentration of CNC in PVA nanocomposite membranes for biogas upgrading application through CO₂ removal. Separation performance was tested at pressure ranges from 5 to 15 bars. Furthermore, membranes were subjected to different % relative humidity's (RH) ranging from 30 to 100% to investigate the effect of swelling on the performance.

2. **Materials**

Commercial polysulfone (PSf) flat sheet ultrafiltration membranes (MWCO 50,000) were purchased from Alfa Laval. Polyvinyl alcohol MW 89000-90000 (89% hydrolyzed) and crystalline nanocellulose (CNC) were purchased from Sigma Aldrich. The average length and the width of CNC was $130 \text{ nm} \pm 67 \text{ nm}$ and $5.9 \text{ nm} \pm 1.8 \text{ nm}$, respectively. Thus the aspect ratio was 23 ± 12 [29]. NaOH was purchased from VWR. De-ionized water was used as main solvent.

2.1. **Casting of FSC membrane**

3 wt. % PVA solution was made by dissolving PVA in deionized water [30]. The clear PVA solution was diluted to 2wt. % with addition of CNC (i.e. 0.5% CNC, 1% CNC, 1.5% CNC, 2% CNC and 4% CNC (wt. % of PVA)) and deionized water. pH's of all the suspensions were adjusted by using 0.1M NaOH. The suspensions were mechanically stirred overnight at room temperature. The viscosities of pure PVA solution and all suspensions with CNC were measured by using rotary type Brook Field viscometer DV2T extra equipped with spindle type V-71 at 25 °C on 250 ml suspension.

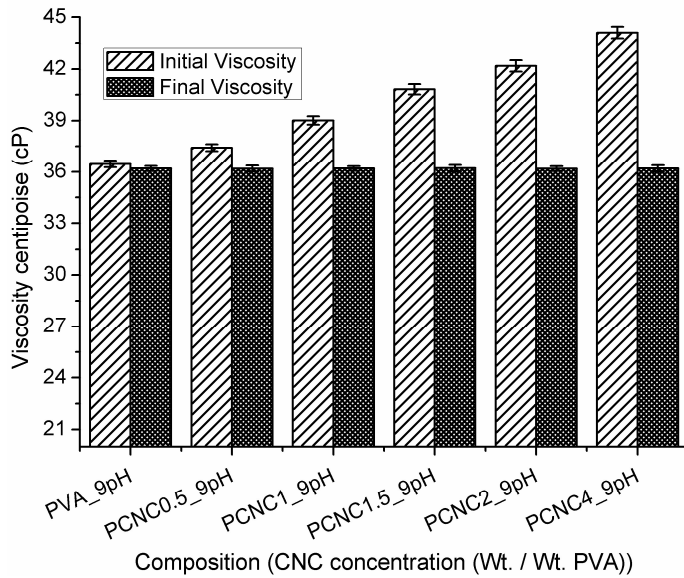


Fig. 1. Viscosity of suspensions before and after dilution with water.

Fig.1 shows the viscosities of suspensions against their concentrations. It is clear that the viscosity of suspensions increased by increasing the concentration of CNC. Deionized water was added to dilute the suspensions until they reached the viscosity of 2% PVA solution. All suspensions were then subjected to ultra-sonication by using a probe sonicator at 60 W for 10 min. The final viscosities of suspensions were measured and plotted against the concentration. The resultant clear suspension was kept standing for 2 hrs at room temperature before casting the membrane. The final compositions of the membranes after dilution are shown in table 1.

Table1: Final concentrations of suspensions after dilution and viscosity adjustment

Membrane type	PVA concentration after dilution	CNC concentration after dilution (Wt. of PVA)

PVA	2%	0%
PCNC0.5	1.96%	0.5%
PCNC1	1.90%	1%
PCNC1.5	1.86%	1.5%
PCNC2	1.81%	2%
PCNC4	1.73%	4%

A nanocomposite membrane containing CNC and PVA were casted to produce a thin dense selective layer over a PSF flat sheet by dip-coating and then subjected to heat treatment according to [11].

2.2. Scanning Electron Microscopy

Membrane morphology was examined by taking cross sectional as well as surface images by scanning electron microscopy (HITACHI SU 3500 SEM). The cross-sectional samples were made by freeze cracking of membranes in liquid nitrogen. Thin gold layer was coated on the samples before observation by using an AGUR auto sputter coater at 35mA for 45 sec. Cross-sectional samples were used to measure the thickness of the selective layer.

2.3. Permeation Test

The separation performance of PVA/CNC nanocomposite membranes were tested in a specially designed high-pressure membrane rig where the feed pressure could be set within the range of 1 – 80 bars [31]. Membranes of different compositions at pH9 were tested for CO₂ permeation and selectivity. A feed gas from the premixed gas cylinder (40 mol% CO₂ and 60 mol% CH₄ gas mixture AGA AS) was supplied to the membrane module. A flat sheet type membrane module was mounted in a thermostatic cabinet with a temperature control system. Experiments were conducted by introducing premixed feed gas in to the membrane

module at 5 different relative humidities (30%, 50%, 70%, 90% and 100% RH) at constant feed pressure of 5 bar. Furthermore, in order to investigate the effect of the feed pressures i.e., 5, 10 and 15 bar the RH was maintained at 100%. All experiments were conducted at constant flow rates of feed and sweep gas streams. The composition of permeate gas was analyzed online by a gas chromatograph.

3. Results and Discussion

3.1. SEM

Different cross-sectional and surface SEM samples were made from each set of membranes. About fifteen SEM images were taken of random areas for each sample. It was observed that membranes after viscosity adjustment of the suspensions have a uniform thickness (0.7 μm to 0.8 μm) and are thinner than the membranes of the same composition but with higher viscosities. Smooth defect free surfaces were observed for all the casted membranes. Fig.2. shows the effect of composition on thickness and SEM cross sectional images of 2wt. % CNC /PVA membranes.

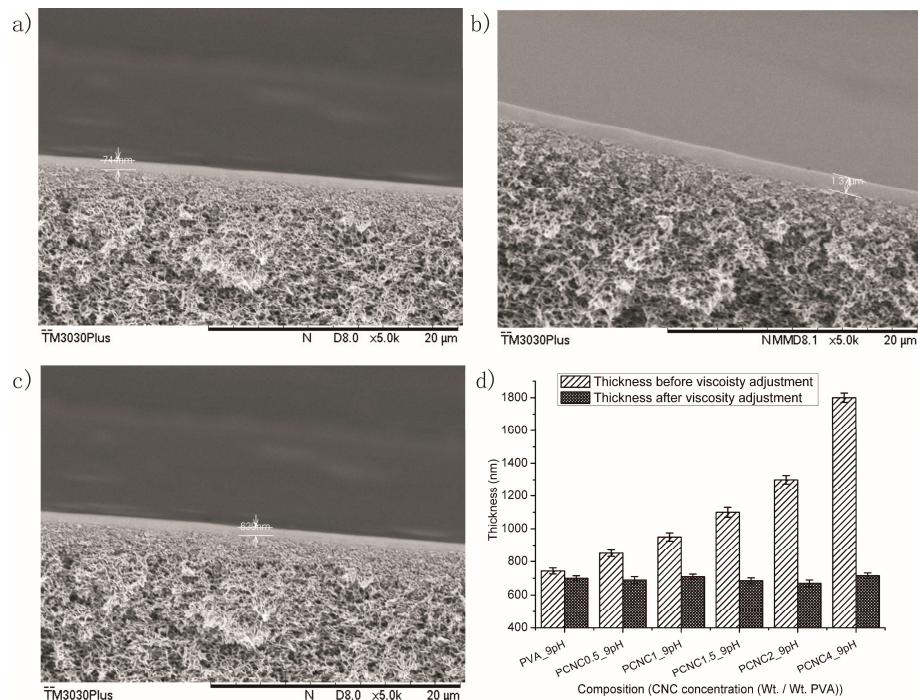


Fig. 2. Thickness and morphology of nanocomposite membranes at different CNC concentrations. (a) cross-sectional view of the pure PVA membrane (b) 2wt.% CNC /PVA membrane before viscosity adjustment of the suspension (c) 2wt.% CNC /PVA membrane after viscosity adjustment of the suspension (d) selective layer thickness compared before and after viscosity adjustment.

3.2. Permeation Test

2wt.% PVA membranes with addition of 0.5wt.%, 1wt.%, 1.5wt.%, 2wt.% and 4wt.% CNC were investigated for their separation performance. Fig.4 illustrates the effect of relative humidity on CO₂ permeance and CO₂/CH₄ selectivity of CNC/PVA nanocomposite membranes with a selective layer of 0.7μm at process conditions of 5 bar and 30 °C. It is evident from the results that the performance of the membranes is improved by increasing RH. However, above 90% RH the improvement in selectivity and permeability is less pronounced. PVA is a hydrophilic polymer and it swells by absorbing moisture from the feed

gas. This water in PVA helps to open up its amorphous domains for mass transfer. The CNC added to PVA improves the swelling of the selective layer somewhat [27]. The increase in the CNC concentration beyond an optimum value causes decrease in the moisture uptake abilities of the selective layer [27]. This decrease at higher nanocellulose concentration may be due to the reinforcing effect of CNC that acts as a reinforcement in the polymer thus restraining swelling mechanically. The swelling data from [27] is plotted against the permeance at 50% RH and 90% RH (Fig. 3).

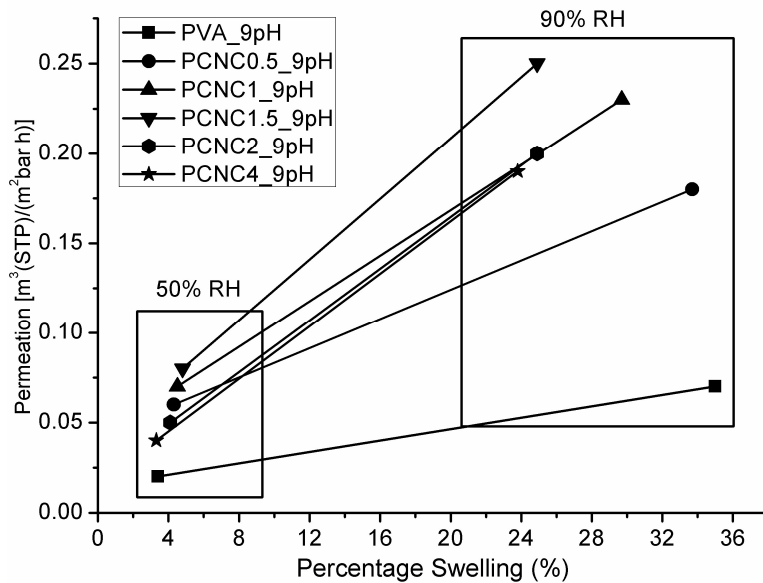


Fig. 3. The swelling data from [27] is plotted against the permeance at 50% RH and 90% RH

Fig. 4 shows that addition of PCNC increases the permeation up to a maximum for 1.5% PCNC addition even when compared at the same swelling in the 90% RH area. This indicates that there must be a different beneficial transport mechanism caused by the nanocellulose than simply affecting total swelling. The characteristics of the strong humidity dependence of CO₂ transport suggested that CO₂ follows the facilitated transport mechanism in water swollen CNC/PVA nano composite membranes.

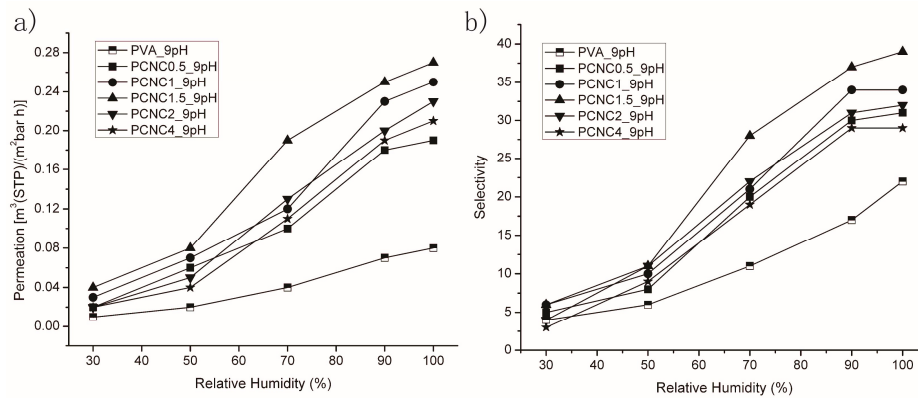


Fig.4. Relationship between relative humidity (RH) and CO₂ permeance for different concentrations of CNC tested at 5 bar. (a) Effect of RH on CO₂ permeance (b) effect of RH on CO₂/CH₄ selectivity

At high RH, membranes absorb more water enhancing CO₂ transport as shown in Fig. 5. In FTM, the CO₂ transport through the membrane is a combined effect of diffusive transport and facilitated transport. The opening of more amorphous regions in highly swollen membranes provides more free volume and pathways for CO₂ transport by diffusion. Secondly, in facilitated transport CO₂ is transported as HCO₃⁻ in water. More water helps to dissociate more CO₂ into bicarbonate ions – this is also pH dependent. These bicarbonate ions are then transported through the membrane. Fig. 4 illustrates the effect of CNC concentration on CO₂ transport through water-swollen membranes. It was observed that 1.5 wt. % CNC at 100% RH has better CO₂ transport properties than all other formulated membranes. For 1.5 wt. % CNC membrane at 30% RH the selectivity was 6 and the permeance was 0.004 m³ (STP)/(m² bar h). Whereas, when RH reaches up to 100% the selectivity was 39 and permeance was 0.27 m³ (STP)/(m² bar h).

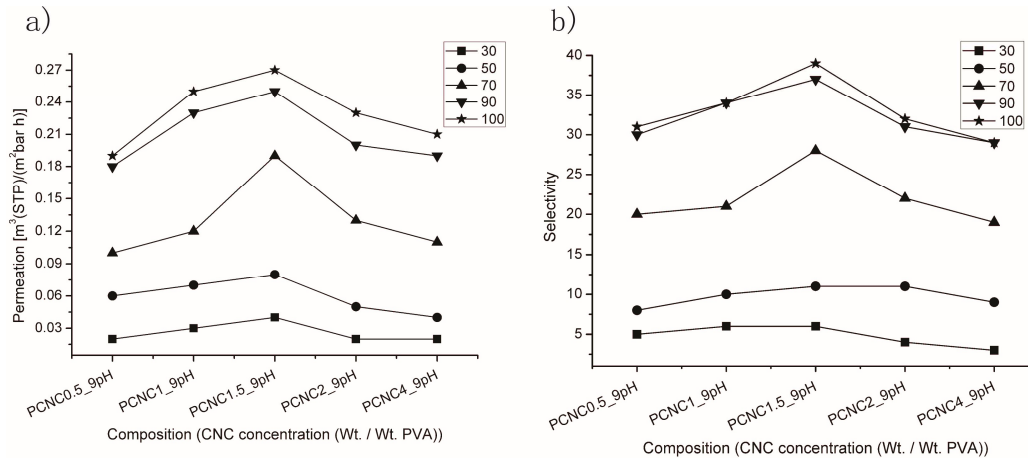


Fig. 5. CNC concentration and membrane performance tested at different relative humidities at feed pressure of 5 bar (a) effect of CNC concentration on CO₂ permeance (b) effect of CNC concentration of CO₂ selectivity

Each membrane has been tested at different pressures 5, 10 and 15 bars. Fig. 6 shows the effect of varying feed pressure on membrane performance. By increasing the pressure both selectivity and permeance decreases for all tested membranes. For 1.5 %CNC, pH 9 at feed pressure of 5 bar, the CO₂/CH₄ selectivity was 39 and the achieved permeance was 0.27 m³(STP)/ (m² bar h). However, at a feed pressure of 15 bars, the selectivity was 31 and permeance decreased to 0.11 m³ (STP)/ (m² bar h). The drop in permeation and selectivity for higher pressure may be due to plasticization and carrier saturation of the polymeric membrane. In facilitated transport, membrane permeance generally decreases with increase in feed pressure. This decrease is more evident at low pressure; once all carriers are saturated only the solution diffusion transport increases with increasing pressure [12]. Additionally, in these membranes decrease in CO₂ permeance could also be a consequence of low water content even at higher RH. High pressure compresses the swollen membrane and results in loss of water and thus a decrease in polymer chain flexibility and free volume for diffusive transport.

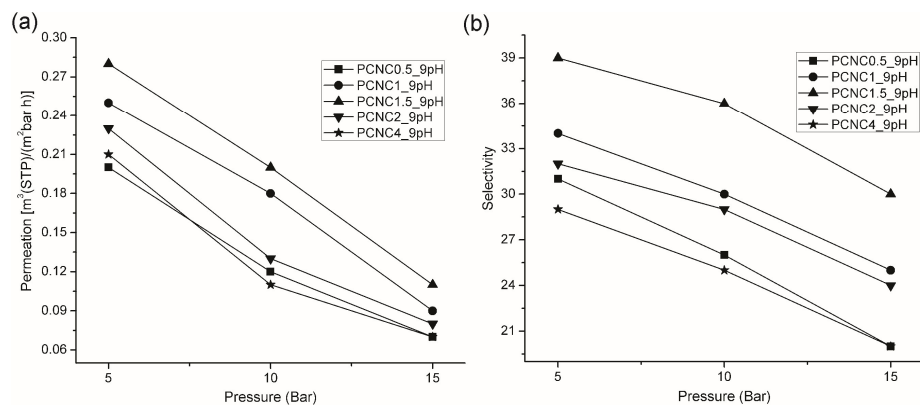


Fig. 6. CO₂ capture at different feed pressures ranging from 5 to 15 bar (a) effect of feed pressure on CO₂ permeance (b) shows the effect of feed pressure on CO₂/CH₄ selectivity

4. Conclusions:

The addition of CNC to PVA has potential for increasing selectivity and permeance considerably. Furthermore, it is also found that higher CNC concentration results in increased thickness of the selective layer after dip coating causing reduced performance of the membrane. Equal thickness membranes can be produced by adjusting the viscosities of the suspensions before casting. PVA membranes containing 1.5% CNC shows remarkably good performance in terms of both selectivity and permeance. Furthermore, increase in RH causes membranes to swell more and hence contributes positively towards increasing CO₂ permeation and CO₂/CH₄ selectivity. When comparing the permeation at same swelling level we see that there is a beneficial effect of CNC addition that cannot be explained by swelling. Increase in feed pressure causes a decrease in both permeation and selectivity – this is a general trend in water swollen membranes.

References

1. Council, N.R., *Advancing the science of climate change. America's Climate Choices: Panel on Advancing the Science of Climate Change*. 2010, Washington, DC: The National Academies Press.
2. Blasing, T., *Recent greenhouse gas concentrations. (32 ndedtn)*. 2012: US department of energy, USA.
3. Atsonios, K., et al., *Exergetic comparison of CO₂ capture techniques from solid fossil fuel power plants*. International Journal of Greenhouse Gas Control, 2016. **45**: p. 106-117.
4. Makaruk, A., M. Miltner, and M. Harasek, *Membrane biogas upgrading processes for the production of natural gas substitute*. Separation and Purification Technology, 2010. **74**(1): p. 83-92.
5. Pires, J.C.M., et al., *Recent developments on carbon capture and storage: An overview*. Chemical Engineering Research & Design, 2011. **89**(9): p. 1446-1460.
6. Zhang, Z., et al., *Progress in enhancement of CO₂ absorption by nanofluids: A mini review of mechanisms and current status*. Renewable Energy, 2018. **118**: p. 527-535.
7. Olajire, A.A., *CO₂ capture and separation technologies for end-of-pipe applications - A review*. Energy, 2010. **35**(6): p. 2610-2628.
8. He, X.Z., C. Fu, and M.B. Hagg, *Membrane system design and process feasibility analysis for CO₂ capture from flue gas with a fixed-site-carrier membrane*. Chemical Engineering Journal, 2015. **268**: p. 1-9.
9. Zhang, Z., *Comparisons of various absorbent effects on carbon dioxide capture in membrane gas absorption (MGA) process*. Journal of Natural Gas Science and Engineering, 2016. **31**: p. 589-595.
10. Kim, T.J., et al., *Separation performance of PVAm composite membrane for CO₂ capture at various pH levels*. Journal of Membrane Science, 2013. **428**: p. 218-224.
11. Saeed, M. and L.Y. Deng, *CO₂ facilitated transport membrane promoted by mimic enzyme*. Journal of Membrane Science, 2015. **494**: p. 196-204.
12. Deng, L.Y., T.J. Kim, and M.B. Hagg, *Facilitated transport of CO₂ in novel PVAm/PVA blend membrane*. Journal of Membrane Science, 2009. **340**(1-2): p. 154-163.
13. Mulder, J., *Basic Principles of Membrane Technology*. 2 ed. 2003, Springer Netherlands: Kluwer Academic Publishers.
14. Yampolskii, Y.F., D.,, *Membrane Gas Separation*. 2011: John Wiley & Sons, Ltd.
15. Mensitieri, G., et al., *The Effect of Film Thickness on Oxygen Sorption and Transport in Dry and Water-Saturated Kapton(R) Polyimide*. Journal of Membrane Science, 1994. **89**(1-2): p. 131-141.
16. Shen, Y. and A.C. Lua, *Effects of membrane thickness and heat treatment on the gas transport properties of membranes based on P84 polyimide*. Journal of applied polymer science, 2010. **116**(5): p. 2906-2912.
17. Firpo, G., et al., *Permeability thickness dependence of polydimethylsiloxane (PDMS) membranes*. Journal of Membrane Science, 2015. **481**: p. 1-8.
18. Koops, G., et al., *Selectivity as a function of membrane thickness: gas separation and pervaporation*. Journal of applied polymer science, 1994. **53**(12): p. 1639-1651.
19. Huang, Y. and D.R. Paul, *Effect of film thickness on the gas-permeation characteristics of glassy polymer membranes*. Industrial & Engineering Chemistry Research, 2007. **46**(8): p. 2342-2347.
20. Ahmad, A.L., S.Y. Olatunji, and Z.A. Jawad, *Thickness Effect on the Morphology and Permeability of CO²/N² Gases in Asymmetric Polyetherimide Membrane*. Journal of Physical Science, 2017. **28**: p. 201.
21. Ansaloni, L., et al., *Nanocellulose-based membranes for CO₂ capture*. Journal of Membrane Science, 2017. **522**: p. 216-225.

22. Cao, X.D. and L.A. Lucia, *Fabrication and properties of cellulose/cellulose nanocrystal composite nanofibers*. Abstracts of Papers of the American Chemical Society, 2010. **239**.
23. Dufresne, A., *Nanocellulose: a new ageless bionanomaterial*. Materials Today, 2013. **16**(6): p. 220-227.
24. Lee, S.Y., et al., *Nanocellulose reinforced PVA composite films: Effects of acid treatment and filler loading*. Fibers and Polymers, 2009. **10**(1): p. 77-82.
25. Habibi, Y., L.A. Lucia, and O.J. Rojas, *Cellulose Nanocrystals: Chemistry, Self-Assembly, and Applications*. Chemical Reviews, 2010. **110**(6): p. 3479-3500.
26. Cho, M.J. and B.D. Park, *Tensile and thermal properties of nanocellulose-reinforced poly(vinyl alcohol) nanocomposites*. Journal of Industrial and Engineering Chemistry, 2011. **17**(1): p. 36-40.
27. Jahan, Z., M.B.K. Niazi, and Ø.W. Gregersen, *Mechanical, thermal and swelling properties of cellulose nanocrystals/PVA nanocomposites membranes*. Journal of Industrial and Engineering Chemistry, 2017.
28. Karaszova, M., et al., *A water-swollen thin film composite membrane for effective upgrading of raw biogas by methane*. Separation and Purification Technology, 2012. **89**: p. 212-216.
29. Molnes, S.N., et al., *Sandstone injectivity and salt stability of cellulose nanocrystals (CNC) dispersions-Premises for use of CNC in enhanced oil recovery*. Industrial Crops and Products, 2016. **93**: p. 152-160.
30. Jahan, Z.N., M.B.K.; Gregersen, O. W.;; *Mechanical, thermal and swelling properties of cellulose nanocrystals/PVA nanocomposites membranes*. Journal of Industrial and Engineering Chemistry, 2017.
31. He, X.Z., T.J. Kim, and M.B. Hagg, *Hybrid fixed-site-carrier membranes for CO₂ removal from high pressure natural gas: Membrane optimization and process condition investigation*. Journal of Membrane Science, 2014. **470**: p. 266-274.

Tables

Table1: Final concentrations of suspensions after dilution and viscosity adjustment

Membrane type	PVA concentration after dilution	CNC concentration after dilution (Wt. of PVA)
PVA	2%	0%
PCNC0.5	1.96%	0.5%
PCNC1	1.90%	1%
PCNC1.5	1.86%	1.5%
PCNC2	1.81%	2%
PCNC4	1.73%	4%

